Mechanical Engineering Advances 2025, 3(1), 2511.
https://doi.org/10.59400/mea2511

Article

Modeling penetration depth in submerged arc welding using artificial neural networks: A comprehensive approach

Farhad Rahmati[1,2,*], Ali Shafipour[2], Masood Aghakhani[2], Farhad Kolahan[1]

[1] Department of Mechanical Engineering, Ferdowsi University of Mashhad, Mashhad 9177948944, Iran
[2] Department of Mechanical Engineering, Razi University, Kermanshah 6714967346, Iran
*** Corresponding author:** Farhad Rahmati, farhadrahmati_24@mail.um.ac.ir

CITATION

Rahmati F, Shafipour A, Aghakhani M, Kolahan F. Modeling penetration depth in submerged arc welding using artificial neural networks: A comprehensive approach. Mechanical Engineering Advances. 2025; 3(1): 2511.
https://doi.org/10.59400/mea2511

ARTICLE INFO

Received: 16 January 2025
Accepted: 20 February 2025
Available online: 27 February 2025

Abstract: Penetration depth, defined as the distance from the surface of the base material to the deepest point of the molten zone, is a critical factor influencing the strength and mechanical properties of welds. This study investigates the effects of process parameters in submerged arc welding (SAW) on penetration depth, utilizing a two-hidden-layer artificial neural network (ANN) for modeling. The input parameters include arc voltage, welding current, electrode stick-out, welding speed, and the thickness of a manganese-enriched nanoparticle layer, with penetration depth as the output variable. The results demonstrate that increasing the welding current to 700 amps enhances heat transfer to the molten pool, thereby improving base material melting and penetration depth. Similarly, raising the arc voltage from 24 to 32 volts results in a moderate increase in penetration depth due to higher heat input while maintaining a relatively stable electrode melting rate. These findings highlight the potential of optimizing SAW parameters to achieve consistent weld quality and desirable mechanical properties.

Keywords: nanoparticles; penetration depth; weld geometry; submerged arc welding; artificial neural networks

1. Introduction

Welding is a versatile and essential process in manufacturing, facilitating the joining of metallic or non-metallic materials to create cohesive and durable structures. As a method that eliminates the need for disassembly, welding provides permanent and robust connections, making it indispensable across diverse industries. Applications range from infrastructure and construction projects to the automotive, aerospace, shipbuilding, and nuclear sectors, where precision and reliability are critical [1–4]. The importance of welding lies not only in its ability to create strong bonds but also in its adaptability to various materials, shapes, and industrial demands. Among the diverse welding techniques, Submerged Arc Welding (SAW) has gained prominence as a specialized and highly efficient method tailored for large-scale and demanding applications. In SAW, the welding arc is formed between a continuously fed electrode wire and the workpiece, with the arc completely submerged under a layer of granular flux. This flux, dispensed from a hopper positioned in front of the electrode, serves multiple functions, including protecting the weld zone from atmospheric contamination, stabilizing the arc, and contributing to the chemical composition of the weld metal [5,6]. The shielding effect of the flux prevents oxidation and other adverse reactions, ensuring a high-quality weld. What sets SAW apart from other welding processes is its efficiency and reliability. With a higher deposition rate compared to conventional methods, SAW allows for faster and more economical welding

operations. This efficiency is coupled with the ability to produce welds that are largely free from defects such as porosity and slag inclusions, which can compromise the structural integrity of the joint. The result is cleaner, stronger welds that meet the rigorous standards of industries requiring high-performance connections [7,8]. SAW is particularly advantageous when welding thicker materials, as it achieves deep penetration and uniform fusion across the joint. Additionally, the controlled heat input and the protective flux layer reduce thermal distortion in the workpiece, a common issue in other welding methods. The process's automation further enhances its appeal by ensuring consistent results, minimizing human error, and boosting overall production efficiency. These features make SAW a preferred choice for applications such as shipbuilding, pipeline construction, and the fabrication of pressure vessels, where precision, durability, and productivity are paramount [9,10]. The quality of welds produced through SAW is determined by evaluating both mechanical properties and geometric characteristics. Mechanical attributes, including tensile strength, hardness, and impact resistance, are critical for ensuring the weld can withstand various stresses and environmental conditions. On the other hand, geometric parameters such as bead height, width, and penetration depth are vital in assessing the weld's structural performance. Among these, penetration depth, which refers to the distance between the surface of the base material and the deepest part of the weld, is particularly significant, as it directly influences the load-bearing capacity and overall strength of the joint. Insufficient penetration can lead to weak bonds, reducing the reliability and safety of the structure [11–15]. Achieving optimal penetration depth in SAW requires precise control of process variables. Key parameters, including welding current, arc voltage, travel speed, and electrode stick-out, collectively determine the heat input, fusion efficiency, and quality of the weld. The interplay between these factors is complex, necessitating advanced methods to analyze and optimize them effectively [16–19]. In recent years, Artificial Neural Networks (ANNs) have emerged as powerful tools for studying and optimizing welding parameters. ANNs are computational models capable of identifying patterns and nonlinear relationships within datasets, making them ideal for understanding the multifaceted interactions in welding processes. By simulating the effects of variables such as current, voltage, and travel speed, ANNs enable researchers to predict welding outcomes with remarkable accuracy. This approach not only reduces the need for extensive experimental trials but also facilitates the identification of optimal parameter settings for specific applications, enhancing the efficiency and reliability of the welding process. In this study, an artificial neural network (ANN) model is applied to analyze the influence of arc voltage, electric current, electrode stick-out, and welding speed on penetration depth. In addition to the standard process parameters, the integration of nanoparticles has emerged as a promising approach to enhancing the microstructure and mechanical properties of welded joints. This novel approach underscores the potential of nanotechnology to address some of the longstanding challenges in welding, particularly in applications requiring superior performance and reliability [20–23]. Consequently, this research also examines the role of a layer of surface-adsorbed Boehmite nanoparticles containing manganese cations, exploring how this additional factor influences the welding process alongside other key parameters.

2. Boehmite nanoparticles

Aluminum oxide, commonly known as alumina, is a white crystalline powder with widespread applications in various industrial fields, including ceramics, refractory materials, and electrotechnology. Among its many phases, Boehmite (γ-AlOOH) stands out as a semi-stable form of aluminum oxide, characterized by the presence of unique surface hydroxyl (OH) groups. These groups facilitate the adsorption of various elements through OH–OH interactions, rendering Boehmite a versatile material for applications involving adsorption and catalysis [24]. The properties of Boehmite nanoparticles are particularly noteworthy due to their combination of chemical stability, superior mechanical strength, and remarkable thermal resistance. They exhibit high catalytic activity, which is further enhanced by their ability to transform into α-alumina, a thermodynamically stable phase, at elevated temperatures [25]. This transformation, combined with the cost-effective synthesis of Boehmite nanoparticles, has positioned them as a material of interest in numerous industrial and scientific endeavors [26]. One of the prominent industrial applications of Boehmite nanoparticles is their role as adsorbents in composite materials, especially in the automotive and oil industries [27]. These nanoparticles have been employed to remove impurities and enhance material properties, owing to their capacity to adsorb metallic cations. In welding processes, for instance, the incorporation of Boehmite nanoparticles enables the adsorption of manganese cations. During welding, the heat facilitates their conversion into alumina and manganese oxide, both of which contribute to the weld pool's properties. This approach offers a low-cost and efficient method to improve the mechanical and chemical characteristics of welded joints. The current study focuses on synthesizing Boehmite nanoparticles and employing them as adsorbents for manganese cations in aqueous media. This process is achieved through a chemical reaction between Boehmite nanoparticles and potassium permanganate ($KMnO_4$) solution. The synthesis method involves a carefully controlled procedure designed to ensure high adsorption efficiency and reproducibility [28,29]. The synthesis begins with the preparation of two distinct solutions. The first solution contains 6.49 g of sodium hydroxide (NaOH) dissolved in 50 mL of distilled water, while the second consists of 20 g of aluminum nitrate nonahydrate ($Al(NO_3)_3 \cdot 9H_2O$) dissolved in 30 mL of distilled water. The NaOH solution is then added dropwise at a rate of 2.94 mm/min to the aluminum nitrate solution, forming a milky suspension. To enhance the uniformity of the reaction, the suspension is subjected to sonication in an ultrasonic bath maintained at 25 ℃ for 3 h. This step ensures the homogeneous distribution of nanoparticles and promotes the formation of the desired Boehmite phase. After sonication, the precipitate is filtered and subsequently dried in an oven at 220 ℃ for 4 h to stabilize the Boehmite nanoparticles. To enable the adsorption of manganese cations onto the synthesized Boehmite nanoparticles, a secondary process is performed. A mixture containing 60 g of Boehmite nanoparticles and 19 g of $KMnO_4$ is dissolved in 400 mL of distilled water. The resulting solution undergoes ultrasonication at 25 ℃ for 15 min to enhance the interaction between the nanoparticles and the potassium permanganate. Following this, the mixture is subjected to reflux at a controlled temperature for 5 h, ensuring sufficient time for the chemical interactions to occur. To complete the process, the solution is stirred

continuously for 24 h, allowing maximum adsorption of manganese cations onto the Boehmite nanoparticle surfaces. This dual-step synthesis and adsorption methodology provides a straightforward yet effective means of enhancing the properties of Boehmite nanoparticles for specific industrial applications. The ability of these nanoparticles to adsorb manganese and subsequently convert into alumina and manganese oxide during high-temperature processes underscores their utility in welding and similar applications. By integrating this approach, it becomes possible to improve the performance and quality of welded materials while keeping production costs low. The synthesis process of boehmite nanoparticles and the formation of crystalline phases are schematically illustrated in **Figure 1**. The diagram includes the preparation of precursors, crystallization at room temperature, formation of the bayerite phase, conversion to the boehmite phase through heating, and the application of ultrasound waves to enhance nanoparticle dispersion.

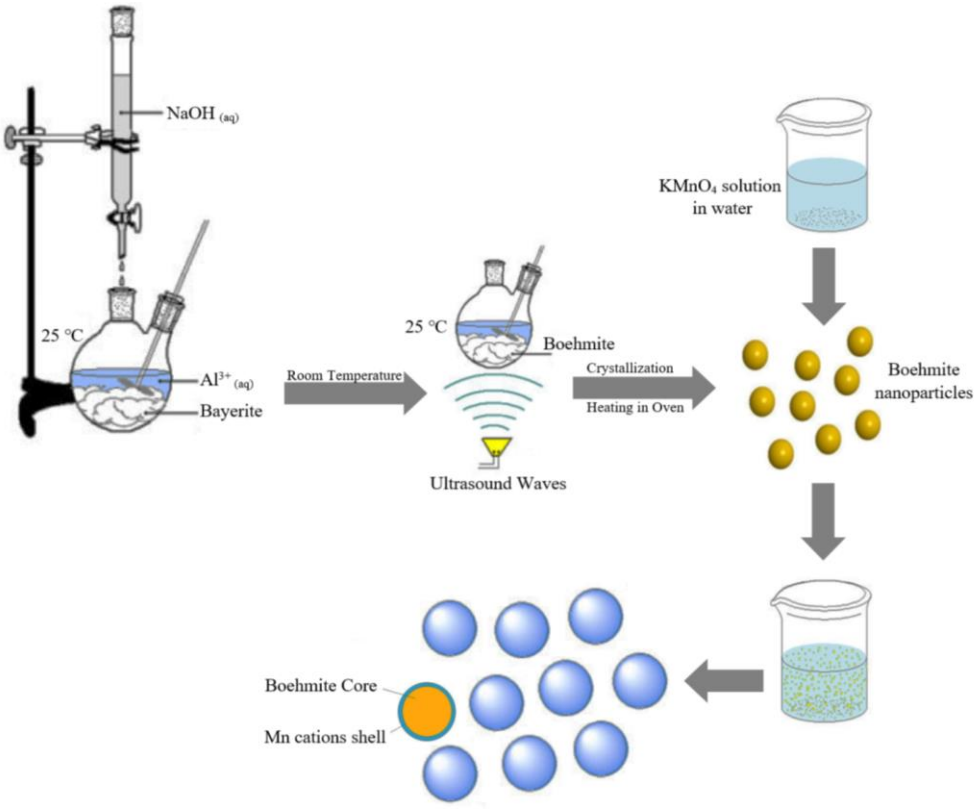

Figure 1. Schematic illustration of boehmite nanoparticle synthesis and crystalline phase formation.

3. Artificial neural network

The Submerged Arc Welding (SAW) process is widely utilized in industrial applications due to its capability to produce high-quality welds with excellent mechanical properties. However, optimizing the process parameters to achieve desired outcomes, such as penetration depth, remains a challenging task. Various factors, including arc voltage, electric current, electrode stick-out, and welding speed, significantly influence the weld quality and characteristics. Modeling the intricate relationships among these parameters is crucial for improving the efficiency and

reliability of the SAW process. Artificial neural networks (ANNs) have emerged as a potent computational tool to model complex systems and nonlinear relationships [30,31]. These systems are inspired by the biological neural networks of the human brain, mimicking their ability to process and analyze data through interconnected layers of nodes or neurons. ANNs have been extensively employed in diverse domains, including image recognition, natural language processing, solving differential equations, and predictive modeling [32,33]. Their adaptability and capability to generalize make them suitable for applications in welding and materials science. A typical ANN structure comprises three main layers: The input layer, one or more hidden layers, and the output layer. The input layer serves as the interface for receiving raw data from the external environment. Each node in this layer corresponds to a specific input parameter. For the SAW process, the input parameters include arc voltage, electric current, electrode stick-out, welding speed, and nanoparticle layer thickness. These parameters are critical as they directly impact the weld penetration and overall quality. The hidden layer, positioned between the input and output layers, plays a central role in processing and analyzing the input data. The number of hidden layers and the nodes within each layer can be customized based on the complexity of the problem. For relatively simple problems, a single hidden layer with a small number of nodes might suffice. However, more intricate relationships demand deeper networks with multiple hidden layers, often requiring greater computational resources. In the context of SAW modeling, the hidden layer processes the input parameters through weighted connections and activation functions, enabling the network to learn and approximate the underlying relationships effectively. The output layer constitutes the final stage of an ANN, producing the model's predictions or classifications. In the present study, the output layer consists of a single node that predicts the penetration depth based on the processed data from the hidden layer. By mapping the input parameters to the desired output, the ANN provides a robust framework for understanding and optimizing the SAW process. The architecture of the ANN used in this research is designed to capture the nonlinear dependencies between the input parameters and the output variable. Specifically, the input layer comprises five nodes representing the aforementioned parameters, while the hidden layer consists of three nodes to balance computational efficiency and modeling accuracy. The connections between the nodes are governed by weights, which are iteratively adjusted during the training phase to minimize the error between the predicted and actual values. This iterative process, known as backpropagation, involves calculating the gradient of the error concerning the weights and updating them accordingly. One of the key advantages of using ANNs for modeling the SAW process is their ability to generalize from training data to unseen scenarios. By leveraging a sufficient dataset that encapsulates a wide range of input-output combinations, the ANN can identify patterns and relationships that are difficult to discern through traditional analytical methods. Moreover, the flexibility of ANNs allows for the incorporation of additional input parameters or the adjustment of network architecture as needed, making them a versatile tool for process optimization.

The current research focuses on utilizing an ANN model to predict the penetration depth during the SAW process. By systematically altering input parameters such as arc voltage, current, electrode stick-out, welding speed, and the

thickness of a nanoparticle layer composed of manganese-containing Boehmite nanoparticles, the model offers critical insights into the underlying process dynamics. The structure of the ANN used in this study, shown in **Figure 2**, demonstrates the arrangement of input, hidden, and output layers specifically designed to address the complexities of the SAW process. This architecture ensures a balance between computational efficiency and prediction accuracy. The findings emphasize the transformative role of ANNs in welding applications, highlighting their capability to manage intricate nonlinear relationships and adapt to varying operational conditions. By offering a robust framework for optimizing process parameters, ANNs significantly enhance the efficiency, quality, and consistency of welds, contributing to the advancement of modern manufacturing methodologies.

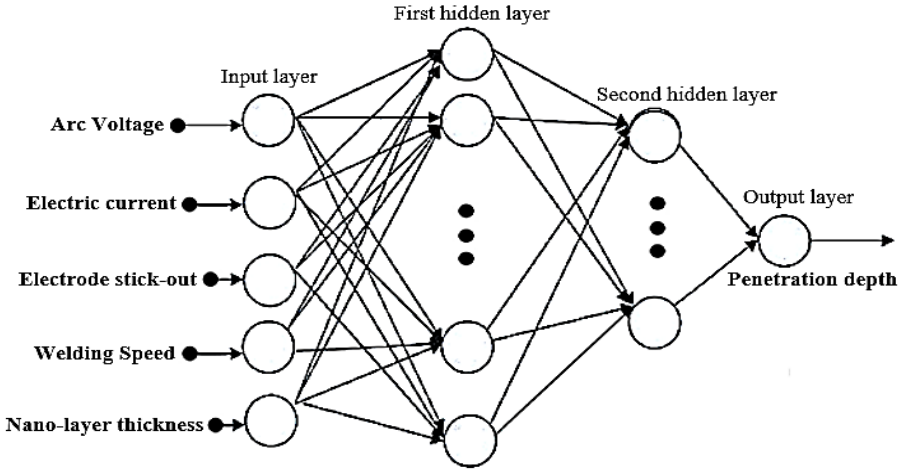

Figure 2. Developed the structure of an artificial neural network model.

4. Experimentation and data collection

ST37 is a mild carbon steel known for its ease of processing and favorable mechanical properties. With a carbon content of approximately 0.17%, this steel is characterized by its ability to maintain a balance between strength and flexibility, making it ideal for a wide range of structural applications. Frequently used in industries such as construction and manufacturing, ST37's qualities make it suitable for components like beams, bridges, and machinery frames that require reliable load-bearing performance. Its excellent weldability further enhances its utility in processes like Submerged Arc Welding (SAW), where achieving robust, durable joints is essential for maintaining long-term structural integrity. In this study, SAW was performed on St37 steel plates, each with dimensions of 15 × 50 × 150 mm^3. The welding operation utilized a direct current (DC) reverse polarity configuration, known for its stability and efficient heat input during the welding process. The setup included a PARS CAT P2310 semi-automatic robotic system, ensuring precision and repeatability throughout the welding operations. The power supply was provided by a PARC ARC 1203T unit, designed with a constant voltage characteristic, which is critical for maintaining consistent weld quality. The consumables used in the welding process comprised a specialized welding wire and flux, whose detailed chemical compositions are provided in **Table 1**. These consumables were carefully selected to

ensure optimal compatibility with the base material and enhance the mechanical properties of the resulting weld joint. In addition, the experimental setup incorporated a layer of Boehmite nanoparticles adsorbed with manganese cations applied to the surface of the base material. This layer was introduced to investigate its potential effects on the welding process and the quality of the weld zone. The key process parameters examined in this investigation included arc voltage, electric current, electrode stick-out length, welding speed, and the thickness of the nanoparticle layer. Preliminary experiments were conducted using a One Variable at a Time (OVAT) approach to establish appropriate ranges for these variables. During these trials, each parameter was varied independently while maintaining all other conditions constant, allowing for the identification of its influence on weld quality. The outcomes of these initial experiments helped define the minimum and maximum values for each parameter, ensuring a systematic and well-controlled experimental design. These ranges are summarized in **Table 2**. Following the determining suitable parameter ranges, a Central Composite Rotatable Design (CCRD) was employed to organize the experimental framework. This statistical method enables a comprehensive evaluation of parameter interactions while minimizing the number of required experiments. The input variables were varied across five levels (−2, −1, 0, +1, and +2), creating a robust design matrix. The matrix and the corresponding experimental results are detailed in **Table 3**. By using this approach, the study aimed to model the complex relationships between the input variables and the welding outcomes, focusing particularly on the depth of weld penetration. Weld penetration depth is a critical factor in ensuring the structural integrity of welded joints, as it directly influences the mechanical performance and load-bearing capacity of the weld. To accurately model this parameter, an artificial neural network (ANN) was implemented. The ANN was trained using the experimental data, enabling it to predict weld penetration depth based on variations in the input parameters. **Figure 3** illustrates the weld-melted zone observed in the prepared workpiece. This zone represents the region where the base material has undergone melting and subsequent solidification during the welding process. The microstructural characteristics of this region are of significant importance, as they directly impact the mechanical properties and long-term performance of the weld. The formation of a uniform and defect-free melted zone is indicative of successful parameter selection and process control.

Table 1. Chemical composition of the wire and flux.

Chemical composition of the welding wire				
Element	C	Mn	Si	Fe
%W	0.04–0.08	0.9–1.3	0.5–0.8	Balance
Chemical composition of the consumed flux				
$SiO_2 + TiO_2$	$Al_2O_3 + MnO$		CaF_2	
% 5	% 55		% 30	

Table 2. Input parameters and their ranges.

Parameter	Coded values				
	−2	**−1**	**0**	**+1**	**+2**
Arc Voltage (volts)	24	26	28	30	32
Electric current (amp)	500	550	600	650	700
Electrode stick-out (mm)	30	32.5	35	37.5	40
Welding Speed (mm/min)	300	350	400	450	500
Nano-layer thickness (mm)	0	0.25	0.5	0.75	1

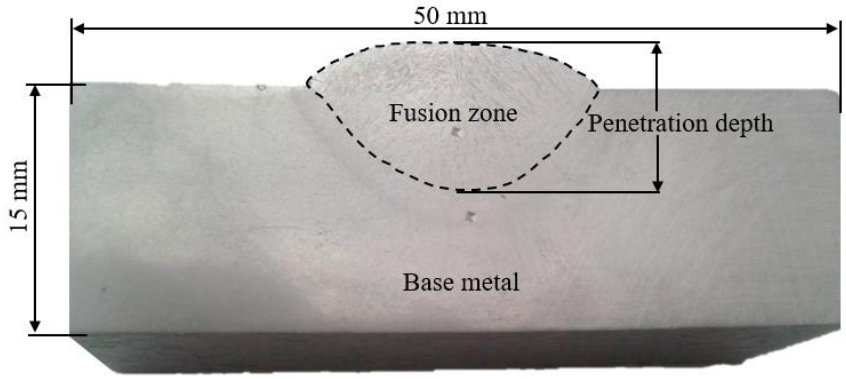

Figure 3. Weld-melted zone in the prepared sample.

Table 3. Input parameters and their ranges.

Std.	Arc voltage (volts)	Electric current (amp)	Electrode stick-out (mm)	Welding speed (mm/min)	Nano-layer thickness (mm)	Penetration depth (mm)	Error
1	28	600	35	400	0.5	7.01	−0.242
2	28	600	35	300	0.5	8.14	0.400
3	26	650	32.5	450	0.75	7.65	0.179
4	26	550	37.5	450	0.75	4.14	−1.363
5	30	650	37.5	350	0.25	9.28	0.363
6	28	700	35	400	0.5	8.80	−0.169
7	30	650	32.5	450	0.25	10.13	1.409
8	28	600	30	400	0.5	7.68	0.312
9	26	550	32.5	350	0.75	5.98	0.090
10	30	650	32.5	350	0.75	8.37	−0.599
11	26	550	37.5	350	0.25	6.09	0.587
12	28	600	35	400	0.5	6.90	−0.352
13	28	600	35	400	0	8.24	0.987
14	26	550	32.5	450	0.25	5.55	−0.129
15	30	550	37.5	450	0.25	5.18	−0.323
16	28	600	35	400	0.5	7.05	−0.202
17	28	600	35	400	0.5	6.89	−0.362
18	26	650	37.5	350	0.75	7.81	−0.207
19	28	600	35	400	1	6.57	−0.188

Table 3. (*Continued*).

Std.	Arc voltage (volts)	Electric current (amp)	Electrode stick-out (mm)	Welding speed (mm/min)	Nano-layer thickness (mm)	Penetration depth (mm)	Error
20	30	650	37.5	450	0.75	8.37	−0.396
21	30	550	32.5	350	0.25	8.14	0.935
22	30	550	37.5	350	0.75	7.29	1.787
23	24	600	35	400	0.5	6.43	−0.823
24	28	600	35	400	0.5	7.27	0.018
25	30	550	32.5	450	0.75	4.62	−0.883
26	28	600	35	400	0.5	6.98	−0.272
27	26	650	32.5	350	0.25	7.75	−0.170
28	26	650	37.5	450	0.25	7.48	0.227
29	28	600	35	500	0.5	6.31	0.094
30	32	600	35	400	0.5	7.89	−0.705
31	28	600	40	400	0.5	6.81	1.307
32	28	500	35	400	0.5	4.64	−0.863
33	28	600	35	300	0.5	8.13	0.316
34	26	650	32.5	450	0.75	7.60	0.149
35	30	650	37.5	350	0.25	9.25	0.193
36	28	700	35	400	0.5	8.75	0.111
37	28	600	30	400	0.5	7.60	0.102
38	26	550	32.5	350	0.75	6.20	0.160
39	26	550	37.5	350	0.25	6.30	0.727
40	28	600	35	400	0.5	6.50	−0.132
41	26	550	32.5	450	0.25	5.70	−0.049
42	30	550	37.5	450	0.25	5.20	−0.333
43	28	600	35	400	0.5	7.10	−0.132
44	26	650	37.5	350	0.75	7.80	−0.327
45	28	600	35	400	1	6.60	−0.068
46	30	650	37.5	450	0.75	8.40	−0.676
47	30	550	37.5	350	0.75	7.30	1.777
48	28	600	35	400	0.5	6.90	−0.132
49	30	550	32.5	450	0.75	4.80	−0.893
50	28	600	35	400	0.5	7.02	−0.132
51	26	650	37.5	450	0.25	7.50	0.227
52	32	600	35	400	0.5	7.80	−0.495
53	28	600	40	400	0.5	6.80	1.257

5. Results and discussion

This study aimed to optimize the penetration depth in Submerged Arc Welding (SAW) by developing a neural network model that links input parameters to the output

variable, which is the penetration depth. The structure of the Artificial Neural Network (ANN) consisted of five neurons in the input layer and one neuron in the output layer. To identify the optimal welding conditions for achieving maximum penetration depth, regression analysis was employed alongside the neural network to evaluate the relationships between the input parameters and the resulting penetration depth. The input parameters included arc voltage, electric current, electrode stick-out, welding speed, and the thickness of the nanoparticle layer, while the output layer represented the penetration depth. For model training, data were randomly selected, and the Levenberg-Marquardt optimization algorithm was applied. A total of 70% of the data was used for training the neural network, adjusting the model based on the calculated error. The remaining 20% was reserved for validating the network, allowing for an assessment of its generalization ability and the cessation of training once further improvements were no longer observed. The final 10% of the data served as the test set, providing an independent measure of the network's performance throughout and after training. **Figure 4** shows an error histogram, representing the distribution of errors for each data group. The regression coefficients comparing the experimental and neural network data for maximizing penetration depth are displayed in **Figure 5**. **Figure 6** illustrates the performance plot of the Artificial Neural Network (ANN) in terms of Mean Squared Error (MSE) and *R*-values, which evaluate the correlation between predicted outputs and target values. The MSE values for the training, validation, and testing datasets were 7.8396×10^{-2}, 5.3101×10^{-2}, and 9.1429×10^{-2}, respectively, highlighting the model's predictive accuracy. A lower MSE value corresponds to better network performance, indicating reduced deviation between predicted and actual values. The *R*-values, reflecting the correlation strength, were 9.9712×10^{-1}, 9.8534×10^{-1}, and 9.6030×10^{-1} for training, validation, and testing, respectively. These values, close to 1, demonstrate a high correlation between network outputs and the target data. The performance plot shows how MSE decreases over 35 epochs for all datasets, with a rapid decline in the initial stages, indicating effective learning. By epoch 29, the network achieves its optimal configuration, as denoted by the circled point labeled "Best." The model exhibits the lowest validation MSE at this point, signifying an optimal balance between accuracy and generalization. The training process halts after six consecutive validation checks without improvement, which prevents overfitting and ensures a robust model. The consistent trend across the training, validation, and testing datasets suggests that the ANN maintains reliability across different data partitions. These findings confirm the network's ability to effectively learn complex input-output relationships and provide accurate predictions for penetration depth in SAW. Additionally, the study explored the influence of various factors, including arc voltage, electric current, electrode stick-out, welding speed, and nanoparticle layer thickness, on the weld penetration depth. **Figure 7** illustrates the influence of various input parameters on penetration depth during the SAW process. The results show that electric current has the most significant impact, with penetration depth increasing markedly as the current rises from 500 to 700 amps due to higher heat input, enhancing base material melting. The results revealed that the intensity of the electric current plays a significant role in determining the welding geometry, as higher current values led to increased penetration depth. This effect is attributed to the greater melting of both the base metal and the welding wire. However,

excessively high currents can result in energy loss and deterioration of the welding wire [34,35]. Arc voltage also contributes to penetration depth, albeit to a lesser extent, with a modest increase observed as the voltage rises from 24 to 32 volts, resulting from slightly higher heat input without substantial changes in electrode melting rate. Electrode stick-out, on the other hand, exhibits an inverse relationship with penetration depth; increasing the distance from 30 to 40 mm reduces heat concentration at the weld pool, leading to shallower penetration. Similarly, welding speed inversely affects penetration depth, with faster speeds (300 to 500 mm/min) reducing the time for heat transfer, thereby diminishing weld penetration [34,35]. Lastly, the addition of nanoparticles reduces penetration depth by decreasing the thermal conductivity of the molten pool, limiting heat transfer to the workpiece as the nano-layer thickness increases.

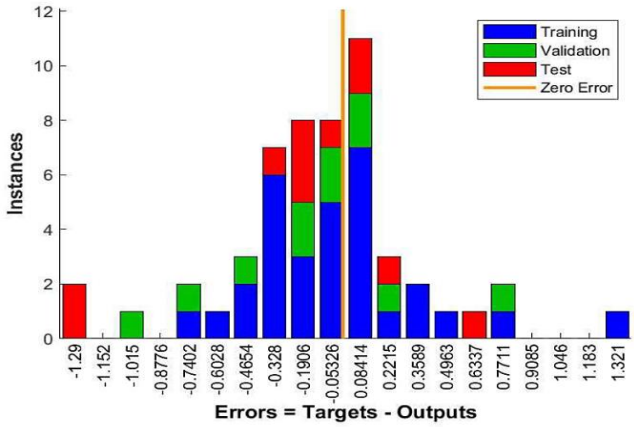

Figure 4. The regression coefficients of experimental data and neural network training data.

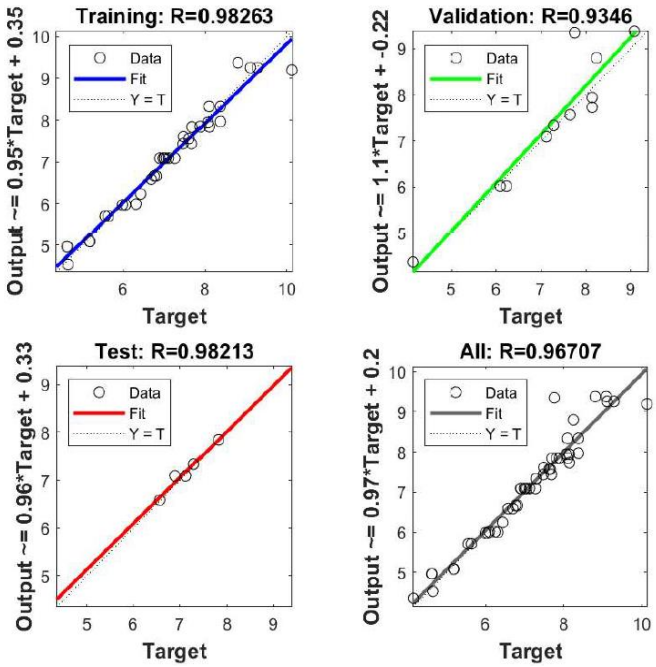

Figure 5. The regression coefficients of experimental data and neural network training data.

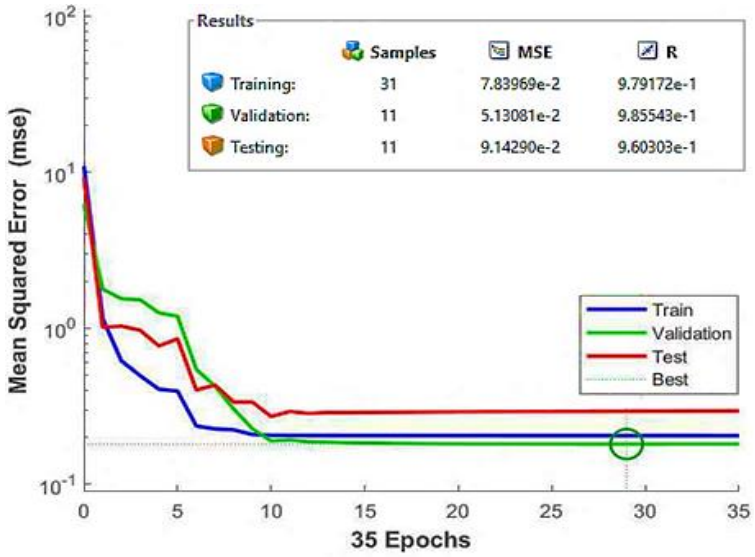

Figure 6. Performance plot: The mean squared error and *R*-values between outputs and target.

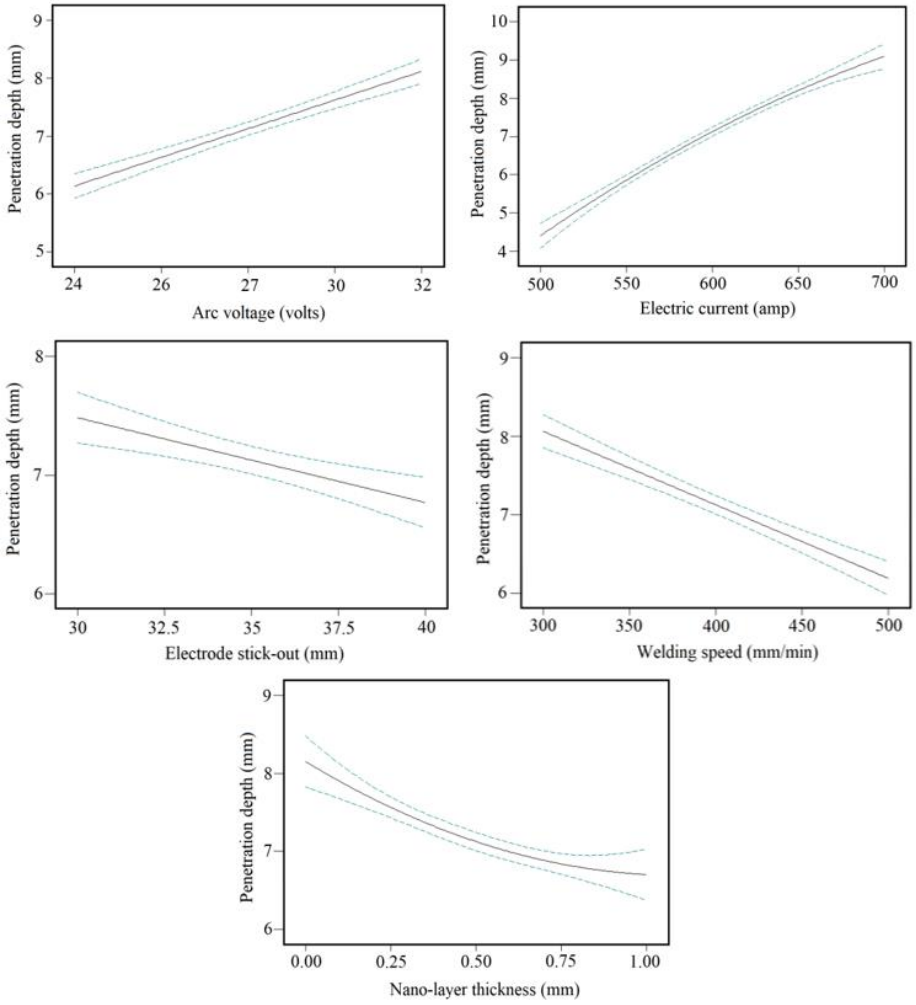

Figure 7. The effect of input parameters on the penetration depth.

6. Conclusions

Submerged Arc Welding (SAW) is a widely employed technique in various industrial sectors, appreciated for its ability to produce strong, defect-free welds. In this research, Artificial Neural Networks (ANNs) were applied to model and optimize penetration depth in the SAW process, addressing the challenges posed by traditional experimental methods. The ANN model provided highly accurate predictions, as demonstrated by low Mean Squared Error (MSE) and high correlation coefficients, verifying its reliability in predicting the effects of input parameters on penetration depth. The study revealed that electric current has the most significant impact on penetration depth, with higher currents increasing heat input and thus enhancing penetration. Arc voltage also contributed to heat transfer, but with a smaller effect. On the other hand, greater electrode stick-out and faster welding speeds were found to decrease penetration depth, as they reduce the concentration of heat in the weld pool. Additionally, the inclusion of nanoparticle layers on the workpiece reduced penetration depth due to their lower thermal conductivity, which limited heat transfer. These findings confirm that ANN-based modeling is a powerful tool for optimizing the SAW process. By offering precise predictions of penetration depth, this approach aids in improving the understanding of key process parameters and can help reduce the need for extensive experimental trials.

Author contributions: Conception and design of the study, FR, AS, MA and FK; prepared the manuscript and conducted data collection and analysis, FR; performed the experiments and collected the data, AS; designed and supervised the project revised the data, and performed the data analysis, MA; analyzed and revised the manuscript, FK. All authors have read and agreed to the published version of the manuscript.

Acknowledgments: The authors would like to thank the Razi University for their assistance throughout the research.

Ethical approval: Not applicable.

Data and code availability: All data used in the paper are cited.

Conflict of interest: The authors declare no conflict of interest.

References

1. Zhang YM, Yang YP, Zhang W, et al. Advanced Welding Manufacturing: A Brief Analysis and Review of Challenges and Solutions. Journal of Manufacturing Science and Engineering. 2020; 142(11). doi: 10.1115/1.4047947
2. Rahmati F, Aghakhani M, Kolahan F. Influence of Siliconized Zn-Graphene Oxide Complex Nanoparticles on the Microstructure and Mechanical Properties of AA5083: Focus on Gas Metal Arc Welding. Advances in Materials Science and Engineering. 2023; 2023: 1-14. doi: 10.1155/2023/3892612
3. Dwivedi DK. Dissimilar Metal Joining. Springer Nature Singapore; 2023. doi: 10.1007/978-981-99-1897-3
4. Rahmati F, Kolahan F, Aghakhani M. Prediction of weld bead geometry of AA5083 using taguchi technique: in the presence of siliconized zn-graphene oxide complex nanoparticles. The International Journal of Advanced Manufacturing Technology. 2024; 136(1): 3-14. doi: 10.1007/s00170-024-13074-0
5. Dwivedi DK. Fundamentals of Metal Joining. Springer Singapore; 2022. doi: 10.1007/978-981-16-4819-9

6. Rathi AK. To study the effect of submerged arc welding parameters on bead geometry and hardness for mild steel (IS-2062A) using fractional factorial design. Materials Today: Proceedings. 2021; 34: 525-530. doi: 10.1016/j.matpr.2020.03.106
7. Patel HN, Chauhan VD, George PM. Effect of process parameters on submerged arc welding: A review. In: Proceedings of the 14th asia-pacific physics conference; 2021. doi: 10.1063/5.0036234
8. Jindal S, Singh M, Chauhan J. Effect and Optimization of Welding Parameters and Flux Baking on Weld Bead Properties and Tensile Strength in Submerged Arc Welding of HSLA 100 Steel. Transactions of the Indian Institute of Metals. 2023; 77(3): 747-766. doi: 10.1007/s12666-023-03158-y
9. Barbosa LHS, Modenesi PJ, Godefroid LB, et al. Fatigue crack growth rates on the weld metal of high heat input submerged arc welding. International Journal of Fatigue. 2019; 119: 43-51. doi: 10.1016/j.ijfatigue.2018.09.020
10. Rajkumar T, Prabakaran MP, Arunkumar G, et al. Evaluation of mechanical and metallurgical properties of submerged arc welded plate joint. Materials Today: Proceedings. 2021; 37: 1367-1371. doi: 10.1016/j.matpr.2020.06.563
11. Choudhary A, Kumar M, Unune DR. Experimental investigation and optimization of weld bead characteristics during submerged arc welding of AISI 1023 steel. Defence Technology. 2019; 15(1): 72-82. doi: 10.1016/j.dt.2018.08.004
12. Kumar R, Dikshit I, Verma A. Experimental investigations and statistical modelling of dilution rate and area of penetration in submerged arc welding of SS316-L. Materials Today: Proceedings. 2021; 44: 3997-4003. doi: 10.1016/j.matpr.2020.10.201
13. Garg J, Garg SB, Jeet B, et al. The effects of flux particle size and column height on the bead geometry in submerged arc welding. Sādhanā. 2022; 47(4). doi: 10.1007/s12046-022-01971-7
14. Mezaache M, Benaouda OF, Kellai A. Maximizing welding efficiency: applying an improved whale optimization algorithm for parametric optimization of bead width in a submerged arc welding process. The International Journal of Advanced Manufacturing Technology. 2024; 134(5-6): 2737-2752. doi: 10.1007/s00170-024-14231-1
15. Shafipour A, Rahmati F, Aghakhani M, et al. Optimization of penetration depth in submerged arc welding using genetic algorithm. The International Journal of Advanced Manufacturing Technology. 2024; 136(1): 123-132. doi: 10.1007/s00170-024-13976-z
16. Sharma H, Rajput B, Singh RP. A review paper on effect of input welding process parameters on structure and properties of weld in submerged arc welding process. Materials Today: Proceedings. 2020; 26: 1931-1935. doi: 10.1016/j.matpr.2020.02.422
17. Sailender M, Reddy GCM, Venkatesh S. Parametric Design for Purged Submerged Arc Welding on Strength of Low Carbon Steel. European Journal of Engineering and Technology Research. 2018; 1(3): 1-6. doi: 10.24018/ejeng.2016.1.3.132
18. Ankush C, Kumar M, Unune DR. Parametric modeling and optimization of novel water-cooled advanced submerged arc welding process. The International Journal of Advanced Manufacturing Technology. 2018; 97(1-4): 927-938. doi: 10.1007/s00170-018-1944-7
19. Vedrtnam A, Singh G, Kumar A. Optimizing submerged arc welding using response surface methodology, regression analysis, and genetic algorithm. Defence Technology. 2018; 14(3): 204-212. doi: 10.1016/j.dt.2018.01.008
20. da Silva MM, Batista VR, Maciel TM, et al. Optimization of submerged arc welding process parameters for overlay welding. Welding International. 2017; 32(2): 122-129. doi: 10.1080/09507116.2017.1347325
21. Choudhary S, Shandley R, Kumar A. Optimization of agglomerated fluxes in submerged arc welding. Materials Today: Proceedings. 2018; 5(2): 5049-5057. doi: 10.1016/j.matpr.2017.12.083
22. Aleshin NP, Grigor'ev MV, Kobernik NV, et al. Modification of Weld Metal with Tungsten Carbide and Titanium Nitride Nanoparticles in Twin Submerged Arc Welding. High Energy Chemistry. 2018; 52(5): 440-445. doi: 10.1134/s0018143918050028
23. Naderian P, Aghakhani M, Khoshboo S. Modelling the hardness of weld metal in the submerged arc welding of low carbon steel plates: addition of CR2O3 nanoparticles. Advances in Materials and Processing Technologies. 2022; 9(1): 221-236. doi: 10.1080/2374068x.2022.2091186
24. Vatanpour V, Madaeni SS, Rajabi L, et al. Boehmite nanoparticles as a new nanofiller for preparation of antifouling mixed matrix membranes. Journal of Membrane Science. 2012; 401-402: 132-143. doi: 10.1016/j.memsci.2012.01.040
25. Jabbari A, Tahmasbi B, Nikoorazm M, et al. A new Pd-Schiff-base complex on boehmite nanoparticles: Its application in Suzuki reaction and synthesis of tetrazoles. Applied Organometallic Chemistry. 2018; 32(6). doi: 10.1002/aoc.4295

26. Ghorbani-Choghamarani A, Seydyosefi Z, Tahmasbi B. Zirconium oxide complex anchored on boehmite nanoparticles as highly reusable organometallic catalyst for C–S and C–O coupling reactions. Applied Organometallic Chemistry. 2018; 32(8). doi: 10.1002/aoc.4396
27. Rajabi L, Derakhshan AA. Room Temperature Synthesis of Boehmite and Crystallization of Nanoparticles: Effect of Concentration and Ultrasound. Science of Advanced Materials. 2010; 2(2): 163-172. doi: 10.1166/sam.2010.1063
28. Ghorbani-Choghamarani A, Seydyosefi Z, Tahmasbi B. Tribromide ion supported on boehmite nanoparticles as a reusable catalyst for organic reactions. Comptes Rendus Chimie. 2018; 21(11): 1011-1022. doi: 10.1016/j.crci.2018.09.001
29. Chen W, Yang T, Dong L, et al. Advances in graphene reinforced metal matrix nanocomposites: Mechanisms, processing, modelling, properties and applications. Nanotechnology and Precision Engineering. 2020; 3(4): 189-210. doi: 10.1016/j.npe.2020.12.003
30. Schrimpf M, Kubilius J, Hong H, et al. Brain-Score: Which Artificial Neural Network for Object Recognition is most Brain-Like?. BioRxiv; 2018. doi: 10.1101/407007
31. Anitescu C, Atroshchenko E, Alajlan N, et al. Artificial Neural Network Methods for the Solution of Second Order Boundary Value Problems. Computers, Materials & Continua. 2019; 59(1): 345-359. doi: 10.32604/cmc.2019.06641
32. Zhao D, Wang Y, Liang D, et al. Performances of regression model and artificial neural network in monitoring welding quality based on power signal. Journal of Materials Research and Technology. 2020; 9(2): 1231-1240. doi: 10.1016/j.jmrt.2019.11.050
33. Sekban DM, Yaylacı EU, Özdemir ME, et al. Investigating Formability Behavior of Friction Stir-Welded High-Strength Shipbuilding Steel using Experimental, Finite Element, and Artificial Neural Network Methods. Journal of Materials Engineering and Performance. 2024. doi: 10.1007/s11665-024-09501-8
34. Karadeniz E, Ozsarac U, Yildiz C. The effect of process parameters on penetration in gas metal arc welding processes. Materials & Design. 2007; 28(2): 649-656. doi: 10.1016/j.matdes.2005.07.014
35. Karaoğlu S, Seçgin A. Sensitivity analysis of submerged arc welding process parameters. Journal of Materials Processing Technology. 2008; 202(1-3): 500-507. doi: 10.1016/j.jmatprotec.2007.10.035